

CMB polarization from secondary vector and tensor modes

Silvia Mollerach

*Centro Atómico Bariloche, Av. Bustillo 9500
8400 Bariloche, Argentina**

Diego Harari

*Departamento de Física, FCEyN, Universidad de Buenos Aires
Ciudad Universitaria - Pab. 1, 1428, Buenos Aires, Argentina†*

Sabino Matarrese

*Dipartimento di Fisica ‘G. Galilei’, Università di Padova
INFN - Sezione di Padova
via Marzolo 8, I-35131 Padova, Italy‡*

(Dated: October 30, 2018)

We consider a novel contribution to the polarization of the Cosmic Microwave Background induced by vector and tensor modes generated by the non-linear evolution of primordial scalar perturbations. Our calculation is based on relativistic second-order perturbation theory and allows to estimate the effects of these secondary modes on the polarization angular power-spectra. We show that a non-vanishing B-mode polarization unavoidably arises from pure scalar initial perturbations, thus limiting our ability to detect the signature of primordial gravitational waves generated during inflation. This secondary effect dominates over that of primordial tensors for an inflationary tensor-to-scalar ratio $r < 10^{-6}$. The magnitude of the effect is smaller than the contamination produced by the conversion of polarization of type E into type B, by weak gravitational lensing. However the lensing signal can be cleaned, making the secondary modes discussed here the actual background limiting the detection of small amplitude primordial gravitational waves.

PACS numbers: 98.70.Vc, 98.80.Es, 98.80.Cq

I. INTRODUCTION

The generation of a stochastic background of primordial gravitational waves is a fundamental prediction of inflationary models for the early Universe. Its amplitude is determined by the energy scale of inflation, which can widely vary between different inflationary models. The detection of this gravitational radiation would provide a crucial test for the validity of the whole scenario. Gravitational wave detectors, however, are quite unlikely to have enough sensitivity to detect such a primordial signal, owing both to its smallness and to its extremely low characteristic frequencies. The existence of ultra-low-frequency gravitational radiation, however, can be indirectly probed thanks to the temperature anisotropy and polarization it induces on the Cosmic Microwave Background (CMB) radiation. In particular, the curl component, called B-mode, of the CMB polarization provides a unique opportunity to disentangle the effect of tensor (gravitational-wave) from scalar perturbations, as this is only excited by either tensor or vector modes [1, 2]. From this point of view, future satellite missions, such as *Planck*, which will have enough sensitivity to either detect or constrain the B-mode CMB polarization predicted by the simplest inflationary models, might represent the first ‘space-based gravitational-wave detector’ [3]. The main complication in this context comes from the effect of gravitational lensing on the CMB by the matter distribution, which implies the transformation of E-mode into B-mode polarization [4]: such a non-linear effect might actually obscure the signal due to primordial tensor modes. It has been pointed out that the inflationary gravitational-wave background can only be detected by CMB polarization measurements if the tensor to scalar ratio $r \geq 10^{-4}$, which corresponds to an energy scale of inflation larger than 3×10^{15} GeV [5, 6, 7, 8]. Quite recently, however, a better technique to *clean* polarization maps from the lensing effect has been proposed, which would allow tensor-to-scalar ratios as low as 10^{-6} , or even smaller, to be probed [9, 10]. Other secondary contributions to the B-type polarization arising during the reionization stage, though of much smaller amplitude, have been considered in [11].

*Electronic address: mollerach@cab.cnea.gov.ar

†Electronic address: harari@df.uba.ar

‡Electronic address: matarrese@pd.infn.it

The case of vector modes is even more interesting, as they cannot be produced during inflation and are in general extremely difficult to generate at early epochs, with the exception of models which predict the existence of primordial tangled magnetic fields [12, 13].

This paper considers a new source of B-mode polarization, coming from secondary vector and tensor modes. The contribution to temperature anisotropy arising from these modes has already been analyzed in Refs. [14, 15]. The evolution of cosmological perturbations away from the linear regime is in fact characterized by mode-mixing, which not only implies that different Fourier modes influence each other, but also that primordial density perturbations act as a source for curl vector perturbations and gravitational waves [43] [16]. Let us emphasize that these secondary vector and tensor modes always exist and that their amplitude has a one-to-one relation with the level of density perturbations, which is severely constrained by both CMB anisotropy measurements and Large-Scale Structure observations. Therefore, their properties are largely inflation model-independent, contrary to primary tensor modes whose amplitude is not only model-dependent, but is well-known to be suppressed in some cases, like e.g. in the so-called *curvaton* model for the generation of curvature perturbations [17].

The plan of the paper is as follows. In Section II we introduce the second-order vector and tensor modes which are produced by the non-linear evolution of primordial scalar perturbations. In Section III we obtain the contribution of these secondary modes to the polarization angular power-spectra, while in Section IV we compare these contributions to those from primordial gravitational waves and gravitational lensing. Section V contains our main conclusions.

II. SECOND-ORDER VECTOR AND TENSOR MODES

The perturbed line-element around a spatially flat FRW background takes a particularly simple form in the so-called Poisson gauge [18], which to linear order reduces to the Newtonian gauge. Adopting the conformal time $d\eta = dt/a$, one can write

$$ds^2 = a^2(\eta) \left\{ - (1 + 2\Psi) d\eta^2 - 2V_i d\eta dx^i + [(1 - 2\Phi) \delta_{ij} + 2H_{ij}] dx^i dx^j \right\} , \quad (1)$$

with δ_{ij} the Kronecker symbol. The lapse perturbation is the sum of a first-order or primary term (indicated by a label P) and a second-order one (indicated by a label S): $\Psi = \Psi_P + \Psi_S$.

The shift perturbation V_i in this gauge is a pure vector, i.e. $\partial^i V_i = 0$, which only arises as a second (or higher)-order contribution (i.e. $V_i = V_{Si}$). The spatial metric perturbations contain a scalar mode, which includes both a linear and a second-order term, $\Phi = \Phi_P + \Phi_S$, and a tensor (i.e. transverse and traceless) mode H_{ij} ($\partial^i H_{ij} = H^i_i = 0$), which also contains first and second-order contributions, namely $H_{ij} = H_{Pi j} + H_{Si j}$. Here and in what follows spatial indices are raised by the Kronecker symbol δ^i_j .

Hereafter we assume that the Universe is spatially flat and filled with a cosmological constant Λ and a pressureless fluid – made of Cold Dark Matter (CDM) plus baryons – whose stress energy-tensor reads $T^\mu_\nu = \rho u^\mu u_\nu$ ($u^\mu u_\mu = -1$). This is a reasonable approximation for the purposes of this paper, although the inclusion of the radiation in the evolution equations would give more accurate results at the smaller scales considered, that entered the horizon during the radiation dominated era.

In this paper we will concentrate on vector and tensor perturbations. In the standard inflationary scenario for the origin of perturbations linear vector modes are not present, but they are generated after horizon crossing as non-linear combinations of primordial scalar modes.

Let us report here the second-order calculation which leads to the generation of these secondary vector and tensor modes. For the $\Lambda = 0$ case, this problem was originally solved in Ref. [16] starting from the results of second-order calculations in the synchronous gauge [19, 20] and transforming them to the Poisson gauge, by means of second-order gauge transformations [21]. Here we will solve the problem directly in the Poisson gauge and we will account for a non-vanishing Λ term (see also [22]).

The background Friedmann equations read $3\mathcal{H}^2 = a^2 (8\pi G\bar{\rho} + \Lambda)$ and $\dot{\rho} = -3\mathcal{H}\bar{\rho}$, where dots indicate differentiation with respect to η , $\mathcal{H} \equiv \dot{a}/a$ and $\bar{\rho}$ is the mean mass-density. Also useful is the relation $2\dot{\mathcal{H}} = -\mathcal{H}^2 + a^2\Lambda$.

We then perturb the mass-density and fluid four-velocity as $\rho = \bar{\rho}(1 + \delta)$ and $u^\mu = (\delta_0^\mu + v^\mu)/a$, with $\delta = \delta_P + \delta_S$ and $v^\mu = v_P^\mu + v_S^\mu$ [16].

Let us briefly report the results of linear perturbation theory in this gauge (for a detailed analysis, see e.g. [23]). The non-diagonal components of i - j Einstein's equations imply $\Psi_P = \Phi_P \equiv \varphi$, for the scalar part, and

$$\ddot{H}_{Pj}^i + 2\mathcal{H}\dot{H}_{Pj}^i - \nabla^2 H_{Pj}^i = 0 , \quad (2)$$

for the tensor part, while its trace gives the evolution equation for the linear scalar potential φ , namely

$$\ddot{\varphi} + 3\mathcal{H}\dot{\varphi} + a^2\Lambda\varphi = 0 . \quad (3)$$

Selecting only the growing-mode solution, we can write $\varphi(\mathbf{x}, \eta) = \varphi_0(\mathbf{x})g(\eta)$, where φ_0 is the peculiar gravitational potential linearly extrapolated to the present time (η_0) and $g = D_+/a$ is the so-called growth-suppression factor, where $D_+(\eta)$ is the linear growing-mode of density fluctuations in the Newtonian limit and a the scale-factor. In the $\Lambda = 0$ case $g = 1$. An excellent approximation for g as a function of redshift z is given in Refs. [24, 25]

$$g \propto \Omega_m \left[\Omega_m^{4/7} - \Omega_\Lambda + (1 + \Omega_m/2)(1 + \Omega_\Lambda/70) \right]^{-1}, \quad (4)$$

with $\Omega_m = \Omega_{0m}(1+z)^3/E^2(z)$, $\Omega_\Lambda = \Omega_{0\Lambda}/E^2(z)$, $E(z) \equiv [\Omega_{0m}(1+z)^3 + \Omega_{0\Lambda}]^{1/2}$ and Ω_{0m} , $\Omega_{0\Lambda} = 1 - \Omega_{0m}$, the present-day density parameters of non-relativistic matter and cosmological constant, respectively. We will normalize the growth-suppression factor so that $g(z=0) = 1$.

The energy and momentum constraints provide the density and velocity fluctuations in terms of φ , namely

$$\begin{aligned} \delta_P &= \frac{1}{4\pi G a^2 \bar{\rho}} \left[\nabla^2 \varphi - 3\mathcal{H}(\dot{\varphi} + \mathcal{H}\varphi) \right], \\ v_{Pi} &= -\frac{1}{4\pi G a^2 \bar{\rho}} \partial_i (\dot{\varphi} + \mathcal{H}\varphi). \end{aligned} \quad (5)$$

Perturbations of the matter stress-energy tensor up to second-order in the Poisson gauge have been calculated in Ref. [26], for a general perfect fluid. Specializing to the pressureless case, one has

$$\begin{aligned} T^0_0 &= -\bar{\rho} (1 + \delta_P + \delta_S + v_P^2), \\ T^i_0 &= -\bar{\rho} [v_P^i + v_S^i + (\varphi + \delta_P) v_P^i], \\ T^0_i &= \bar{\rho} [v_{Pi} + v_{Si} - V_i + (-3\varphi + \delta_P) v_{Pi}], \\ T^i_j &= \bar{\rho} v_P^i v_{Pj}, \end{aligned} \quad (6)$$

where $v_P^2 \equiv v_P^j v_{Pj}$. Note that the second-order velocity v_{Si} is the sum of an irrotational component $v_{Si}^{(0)}$, which is the gradient of a scalar, and a rotational vector $v_{Si}^{(1)}$, which has zero divergence, $\partial^i v_{Si}^{(1)} = 0$.

For the purpose of obtaining secondary vector and tensor modes, we can start by writing the second-order momentum-conservation equation [44], $T^{\mu}_{i;\mu} = 0$, which gives

$$\left(\dot{v}_{Si}^{(1)} - \dot{V}_i \right) + \mathcal{H} \left(v_{Si}^{(1)} - V_i \right) = -\partial_i \Psi_S - 2\dot{\varphi} v_{Pi} - \frac{1}{2} \partial_i (v_P^2 + \varphi^2). \quad (7)$$

For pure growing-mode initial conditions $\dot{\varphi} \propto \varphi$ and $v_{Pi} \propto \partial_i \varphi$, which makes the RHS of this equation the gradient of a scalar quantity; thus, the vector part only contains a decaying solution $(v_{Si}^{(1)} - V_i) \propto a^{-1}$, and we can safely assume $v_{Si}^{(1)} = V_i$.

To proceed one needs the second-order perturbations of the Einstein tensor, $\delta^{(2)} G^{\mu}_{\nu}$: these can be found for any gauge in Appendix A of Ref. [27].

The second-order ‘momentum constraint’ $\delta^{(2)} G^i_0 = 8\pi G \delta^{(2)} T^i_0$ gives

$$\partial^i \left(\mathcal{H} \Psi_S + \dot{\Phi}_S \right) + \frac{1}{4} \nabla^2 V^i + \dot{\varphi} \partial^i \varphi + 4\varphi \partial^i \dot{\varphi} = -4\pi G a^2 \bar{\rho} \left[(\varphi + \delta_P) v_P^i + v_S^{(0)i} \right]. \quad (8)$$

The pure vector part of this equation can be isolated by first taking its divergence to solve for the combination $\mathcal{H} \Psi_S + \dot{\Phi}_S$ and then replacing it in the original equation. We obtain

$$\nabla^2 \nabla^2 V_i = 16\pi G a^2 \bar{\rho} \partial^j (v_{Pj} \partial_i \delta_P - v_{Pi} \partial_j \delta_P). \quad (9)$$

We can further simplify this equation and write:

$$\nabla^2 V_i = -\frac{8}{3} F(z) \left(\partial_i \varphi_0 \nabla^2 \varphi_0 - \partial^i \partial^j \varphi_0 \partial_j \varphi_0 + 2\partial_j \Theta_0 \right), \quad (10)$$

with

$$F(z) = \frac{2g^2(z)E(z)f(\Omega_m)}{\Omega_{0m}H_0(1+z)^2},$$

where [24, 25] $f(\Omega_m) \equiv d \ln D_+ / d \ln a \approx \Omega_m(z)^{4/7}$, H_0 is the Hubble constant and

$$\nabla^2 \Theta_0 = -\frac{1}{2} \left((\nabla^2 \varphi_0)^2 - \partial_i \partial_k \varphi_0 \partial^i \partial^k \varphi_0 \right). \quad (11)$$

For $\Lambda = 0$, the above expression for V_i reduces to Eq. (6.8) of Ref. [16], noting that $F(z) = \eta$ in that case.

Finally, we can solve for the second-order tensor modes by looking at the traceless part of i - j Einstein's equations, $\delta^{(2)} G^i_j - \frac{1}{3} \delta^{(2)} G^k_k \delta_j^i = 8\pi G (\delta^{(2)} T^i_j - \frac{1}{3} \delta^{(2)} T^k_k \delta_j^i)$, namely

$$\begin{aligned} & - \left[\frac{1}{3} \nabla^2 (\Phi_S - \Psi_S) + \frac{2}{3} (\nabla \varphi)^2 + \frac{4}{3} \varphi \nabla^2 \varphi \right] \delta_j^i + \partial^i \partial_j (\Phi_S - \Psi_S) + 2 \partial^i \varphi \partial_j \varphi + 4 \varphi \partial^i \partial_j \varphi \\ & + \frac{1}{2} \left(\partial^i \dot{V}_j + \partial_j \dot{V}^i \right) + \mathcal{H} (\partial^i V_j + \partial_j V^i) + \left(\ddot{H}_{Sj}^i + 2\mathcal{H} \dot{H}_{Sj}^i - \nabla^2 H_{Sj}^i \right) = 8\pi G a^2 \bar{\rho} \left(v_{\text{P}j}^i v_{\text{P}j} - \frac{1}{3} v_{\text{P}}^2 \delta_j^i \right). \end{aligned} \quad (12)$$

To deal with this equation, we first apply the operator $\partial^i \partial_i$, which allows to solve for the combination $\Phi_S - \Psi_S$, and then replace it in the original equation, together with the expression for the vector mode V_i . After a lengthy but straightforward calculation we obtain

$$\nabla^2 \nabla^2 \left(\ddot{H}_{Sj}^i + 2\mathcal{H} \dot{H}_{Sj}^i - \nabla^2 H_{Sj}^i \right) = \nabla^2 \partial^k \partial_\ell R_k^\ell \delta_j^i + 2 \nabla^2 \left(\nabla^2 R^i_j - \partial^i \partial_k R^k_j - \partial^k \partial_j R^i_k \right) + \partial^i \partial_j \partial^k \partial_\ell R_k^\ell, \quad (13)$$

where we introduced the traceless tensor

$$\begin{aligned} R_k^\ell & \equiv \partial^\ell \varphi \partial_k \varphi - \frac{1}{3} (\nabla \varphi)^2 \delta_k^\ell + 4\pi G a^2 \bar{\rho} \left(v_{\text{P}k}^\ell v_{\text{P}k} - \frac{1}{3} v_{\text{P}}^2 \delta_k^\ell \right) \\ & = g^2 \left(1 + \frac{2E^2(z) f^2(\Omega_m)}{3\Omega_{0m}(1+z)^3} \right) \left(\partial^\ell \varphi_0 \partial_k \varphi_0 - \frac{1}{3} (\nabla \varphi_0)^2 \delta_k^\ell \right). \end{aligned} \quad (14)$$

Equation (13) can be solved by Green's method, as the corresponding homogeneous equation is the one for linear tensor modes, whose analytical solutions are known in the limiting cases $\Omega_m \rightarrow 1$ or $\Omega_\Lambda \rightarrow 1$. In the $\Lambda \rightarrow 0$ limit one recovers the result of Ref. [16], namely

$$H_{Sij}(\mathbf{x}, \eta) = \frac{1}{(2\pi)^3} \int d^3 k e^{i\mathbf{k} \cdot \mathbf{x}} \frac{40}{k^4} \mathcal{S}_{ij}(\mathbf{k}) \left(\frac{1}{3} - \frac{j_1(k\eta)}{k\eta} \right), \quad (15)$$

where j_ℓ are spherical Bessel functions of order ℓ and $\mathcal{S}_{ij}(\mathbf{k}) = \int d^3 y e^{-i\mathbf{k} \cdot \mathbf{y}} \mathcal{S}_{ij}(\mathbf{y})$, with

$$\mathcal{S}_{ij} = \nabla^2 \Theta_0 \delta_{ij} + \partial_i \partial_j \Theta_0 + 2 \left(\partial_i \partial_j \varphi_0 \nabla^2 \varphi_0 - \partial_i \partial_k \varphi_0 \partial^k \partial_j \varphi_0 \right). \quad (16)$$

For the purpose of the present analysis, the main contribution comes from the early evolution of H_{Sij} , when the cosmological constant term can be neglected. One can then adopt the Einstein-de Sitter result above, up to an overall correction factor $g_\infty^2 \equiv g^2(z \rightarrow \infty)$.

It proves convenient to express the previous quantities in Fourier space. Let us define

$$V_j(\mathbf{x}, \eta) = \frac{1}{(2\pi)^3} \int d^3 k \left[V^{(+1)}(\mathbf{k}, \eta) Q_j^{(+1)}(\mathbf{k}, \mathbf{x}) + V^{(-1)}(\mathbf{k}, \eta) Q_j^{(-1)}(\mathbf{k}, \mathbf{x}) \right], \quad (17)$$

where [29]

$$Q_j^{(\pm 1)}(\mathbf{k}, \mathbf{x}) = \frac{i}{\sqrt{2}} (\hat{\mathbf{e}}_1 \pm i \hat{\mathbf{e}}_2)_j \exp(i\mathbf{k} \cdot \mathbf{x}), \quad (18)$$

with $\hat{\mathbf{e}}_1$, $\hat{\mathbf{e}}_2$ and $\hat{\mathbf{e}}_3 = \hat{\mathbf{k}}$ forming an orthonormal basis and

$$V^{(\pm 1)}(\mathbf{k}, \eta) = \frac{\sqrt{2} F(z)}{3 k^2} \int \frac{d^3 k'}{(2\pi)^3} (\hat{\mathbf{e}}_1 \mp i \hat{\mathbf{e}}_2) \cdot \mathbf{k}' (k^2 - 2\mathbf{k} \cdot \mathbf{k}') \varphi_0(\mathbf{k}') \varphi_0(\mathbf{k} - \mathbf{k}'). \quad (19)$$

The peculiar gravitational potential φ_0 is a Gaussian random field with Fourier space correlation

$$\langle \varphi_0(\mathbf{k}) \varphi_0(\mathbf{k}') \rangle = (2\pi)^3 \delta^{(3)}(\mathbf{k} + \mathbf{k}') P_\varphi(k), \quad (20)$$

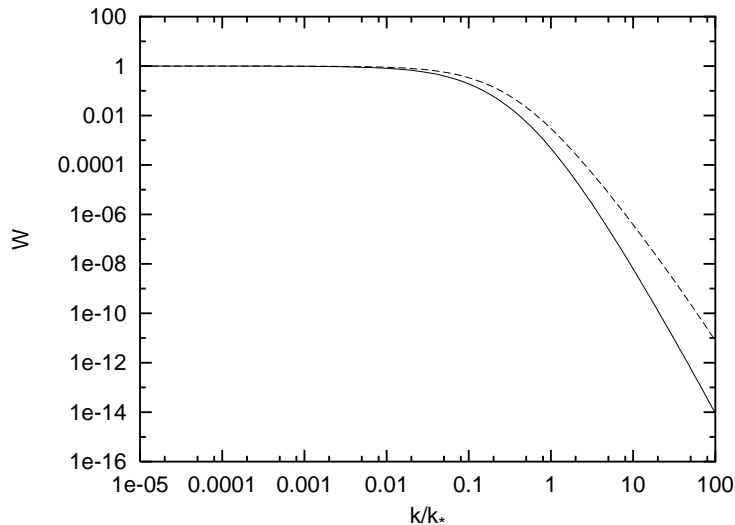


FIG. 1: The functions W_V (dashed line) and W_χ (solid line) for $n_s = 1$.

where $P_\varphi(k)$ is the gravitational potential power-spectrum $P_\varphi(k) = P_{0\varphi}k^{-3}(k/k_0)^{n_s-1}T_s^2(k)$, k_0 is some pivot wavenumber and T_s is the usual matter transfer function [30], which is unity on large scales and drops off like k^{-2} on small scales because of the stagnation effect of matter perturbations on sub-horizon scales during radiation dominance. For later convenience we can relate P_φ to the dimensionless power-spectrum of the comoving curvature perturbation (see e.g. [31]) \mathcal{R} , namely $\Delta_{\mathcal{R}}^2(k) = \Delta_{\mathcal{R}}^2(k_0)(k/k_0)^{n_s-1}$, where $\Delta_{\mathcal{R}}^2(k_0) = (25/9)(P_{0\varphi}/2\pi^2)$ [45].

The vectors $V^{(\pm 1)}$ are two independent, *chi-square* distributed random fields each one with power-spectrum

$$P_V(k, \eta) = \frac{1}{9\pi^2} \frac{F(z)^2}{k^4} \int_{-1}^1 d\cos\theta (1 - \cos^2\theta) \int_0^\infty dk' k'^4 (k^2 - 2kk' \cos\theta)^2 P_\varphi(k') P_\varphi(\sqrt{k'^2 + k^2 - 2k'k \cos\theta}), \quad (21)$$

which, after numerical integration yields

$$P_V(k) = \frac{36\pi^2}{(25)^2} C_V(n_s) \Delta_{\mathcal{R}}^4(k_0) (kF(z))^2 k^{-3} \left(\frac{k}{k_*}\right)^{-1} \left(\frac{k_*}{k_0}\right)^{2(n_s-1)} W_V(k/k_*), \quad (22)$$

where $k_* = \Omega_{0m}h^2 \text{ Mpc}^{-1}$, with h the Hubble constant H_0 in units of $100 \text{ km s}^{-1} \text{ Mpc}^{-1}$; the coefficient $C_V(n_s)$ ranges from 0.062 to 0.29 for n_s between 1 and 0.8, respectively. The function $W_V(x)$ (which is also weakly dependent on n_s) is unity for $x \ll 1$ and drops to zero at $x \approx 1$; its form is plotted in Figure 1 (for $n_s = 1$). A good fit, useful for next section calculations, is given by $W_V(x) = (1 + 5x + 3x^2)^{-5/2}$.

For tensor modes we similarly define

$$H_{ij}(\mathbf{x}, \eta) = \frac{1}{(2\pi)^3} \int d^3k \left[H^{(+2)}(\mathbf{k}, \eta) Q_{ij}^{(+2)}(\mathbf{k}, \mathbf{x}) + H^{(-2)}(\mathbf{k}, \eta) Q_{ij}^{(-2)}(\mathbf{k}, \mathbf{x}) \right], \quad (23)$$

where [29]

$$Q_{ij}^{(\pm 2)}(\mathbf{k}, \mathbf{x}) = -\sqrt{\frac{3}{8}} (\hat{\mathbf{e}}_1 \pm i\hat{\mathbf{e}}_2)_i (\hat{\mathbf{e}}_1 \pm i\hat{\mathbf{e}}_2)_j \exp(i\mathbf{k} \cdot \mathbf{x}). \quad (24)$$

The primary tensor modes can be expressed as

$$H_P^{(\pm 2)}(\mathbf{k}, \eta) = \chi_P^{(\pm 2)}(\mathbf{k}) \frac{3j_1(k\eta)}{k\eta}, \quad (25)$$

for the Einstein-de Sitter case, where $\chi_P^{(+2)}$ and $\chi_P^{(-2)}$ are two independent Gaussian fields each one with power-spectrum $P_{\chi_P}(k) = P_{0\chi_P}k^{-3}(k/k_0)^{n_t}T_t^2(k)$. The tensor transfer function $T_t(k)$ reads $T_t(k) = [1 + 1.34y + 2.5y^2]^{1/2}$ [32], where $y \equiv k/k_{\text{eq}}$ and $k_{\text{eq}} = 0.073\Omega_{0m}h^2 \text{ Mpc}^{-1}$ is the horizon scale at matter radiation equality. In the $\Lambda \neq 0$ case the evolution of primary tensor modes is more complicated and will be dealt with using CMBFAST [33].

We can similarly relate $P_{\chi_P}(k)$ to the dimensionless tensor power-spectrum (see e.g. [31]), $\Delta_t^2(k) = \Delta_t^2(k_0)(k/k_0)^{n_t}$, where $\Delta_t^2(k_0) = (P_{0\chi_P}/2\pi^2)$. Defining the ‘tensor-to-scalar’ ratio as in Ref. [31], we find

$$r \equiv 24 \frac{\Delta_t^2(k_0)}{\Delta_{\mathcal{R}}^2(k_0)}. \quad (26)$$

In single-field slow-roll inflation models the standard consistency relation $n_t = -r/8$ also applies [34].

The secondary tensor modes are instead characterized by

$$H_S^{(\pm 2)}(\mathbf{k}, \eta) \approx \left(1 - \frac{3j_1(k\eta)}{k\eta}\right) g_\infty^2 \chi_S^{(\pm 2)}(\mathbf{k}), \quad (27)$$

where we have introduced the factor g_∞^2 that makes this a good approximation in the $\Lambda \neq 0$ case for $z > \text{few}$ as discussed above. The secondary tensors in Eq. (27) are given by

$$\chi_S^{(\pm 2)}(\mathbf{k}) = \frac{10}{3\sqrt{6}k^2} \int \frac{d^3k'}{(2\pi)^3} [\mathbf{k}' \cdot (\hat{\mathbf{e}}_1 \mp \hat{\mathbf{e}}_2)]^2 \varphi_0(\mathbf{k}') \varphi_0(\mathbf{k} - \mathbf{k}'), \quad (28)$$

and are *chi-square* distributed independent random fields with power-spectra

$$P_{\chi_S}(k) = \frac{25}{27\pi^2} \frac{1}{k^4} \int_{-1}^1 d\cos\theta \sin^4\theta \int_0^\infty dk' k'^6 P_\varphi(k') P_\varphi(\sqrt{k'^2 + k^2 - 2k'k\cos\theta}), \quad (29)$$

which can be numerically integrated to give

$$P_{\chi_S} = \frac{12\pi^2}{25} C_{\chi_S} \Delta_{\mathcal{R}}^4(k_0) k^{-3} \left(\frac{k}{k_*}\right)^{-1} \left(\frac{k_*}{k_0}\right)^{2(n_s-1)} W_{\chi_S}(k/k_*), \quad (30)$$

where the coefficient $C_{\chi_S}(n_s)$ ranges from 0.062 to 0.29 for n_s between 1 and 0.8, respectively. The function $W_{\chi_S}(x)$ (which weakly depends on n_s) is unity for $x \ll 1$ and drops to zero at $x \approx 1$; its form is also plotted in Figure 1 (for $n_s = 1$). It can be well fitted by $W_\chi(x) = (1 + 7x + 5x^2)^{-3}$.

III. POLARIZATION ANGULAR POWER-SPECTRA

Polarization of the CMB arises from Thomson scattering of anisotropic radiation by free electrons. The generation of temperature and polarization anisotropies in the CMB from gravitational perturbations has been studied in detail by several authors [1, 2, 29, 35]. A simple and powerful formalism is the total angular momentum method [29, 35], which includes the effect of scalar, vector and tensor modes on an equal footing. This is the most convenient approach for our calculations, and we are going to extensively use the results of Ref. [29]. The temperature and polarization fluctuations are expanded in normal modes that take into account the dependence on both the angular direction of photon propagation \mathbf{n} and the spatial position \mathbf{x} , ${}_s G_\ell^m(\mathbf{x}, \mathbf{n})$

$$\begin{aligned} \Theta(\eta, \mathbf{x}, \mathbf{n}) &= \int \frac{d^3k}{(2\pi)^3} \sum_\ell \sum_{m=-2}^2 \Theta_\ell^{(m)} {}_0 G_\ell^m, \\ (Q \pm iU)(\eta, \mathbf{x}, \mathbf{n}) &= \int \frac{d^3k}{(2\pi)^3} \sum_\ell \sum_{m=-2}^2 (E_\ell^{(m)} \pm iB_\ell^{(m)}) {}_{\pm 2} G_\ell^m, \end{aligned} \quad (31)$$

with spin $s = 0$ describing the temperature fluctuation and $s = \pm 2$ describing the polarization tensor and $m = 0, \pm 1, \pm 2$ denoting scalar, vector and tensor perturbations, respectively. $E_\ell^{(m)}$ and $B_\ell^{(m)}$ are the angular moments of the electric and magnetic polarization components and

$${}_s G_\ell^m(\mathbf{x}, \mathbf{n}) = (-i)^\ell \sqrt{\frac{4\pi}{2\ell+1}} [{}_s Y_\ell^m(\mathbf{n})] \exp(i\mathbf{k} \cdot \mathbf{x}). \quad (32)$$

The Boltzmann equation describing the time evolution of the radiation distribution under gravitation and scattering processes can be written as a set of evolution equations for the angular moments of the temperature, $\Theta_\ell^{(m)}$ (for $\ell \geq m$),

and both polarization types, $E_\ell^{(m)}$ and $B_\ell^{(m)}$ (for $\ell \geq 2$ and $m \geq 0$),

$$\dot{\Theta}_\ell^{(m)} = k \left[\frac{0\kappa_\ell^m}{(2\ell-1)} \Theta_{\ell-1}^{(m)} - \frac{0\kappa_{\ell+1}^m}{(2\ell+3)} \Theta_{\ell+1}^{(m)} \right] - \dot{\tau} \Theta_\ell^{(m)} + S_\ell^{(m)}, \quad (33)$$

$$\dot{E}_\ell^{(m)} = k \left[\frac{2\kappa_\ell^m}{(2\ell-1)} E_{\ell-1}^{(m)} - \frac{2m}{\ell(\ell+1)} B_\ell^{(m)} - \frac{2\kappa_{\ell+1}^m}{(2\ell+3)} E_{\ell+1}^{(m)} \right] - \dot{\tau} [E_\ell^{(m)} + \sqrt{6} P^{(m)} \delta_{\ell,2}], \quad (34)$$

$$\dot{B}_\ell^{(m)} = k \left[\frac{2\kappa_\ell^m}{(2\ell-1)} B_{\ell-1}^{(m)} + \frac{2m}{\ell(\ell+1)} E_\ell^{(m)} - \frac{2\kappa_{\ell+1}^m}{(2\ell+3)} B_{\ell+1}^{(m)} \right] - \dot{\tau} B_\ell^{(m)}, \quad (35)$$

where the coupling coefficients are

$${}_s \kappa_\ell^m = \sqrt{\frac{(\ell^2 - m^2)(\ell^2 - s^2)}{\ell^2}}. \quad (36)$$

The fluctuation sources are given by

$$\begin{aligned} S_0^{(0)} &= \dot{\tau} \Theta_0^{(0)} - \dot{\Phi}, & S_1^{(0)} &= \dot{\tau} v_B^{(0)} + k \Psi, & S_2^{(0)} &= \dot{\tau} P^{(0)}, \\ S_1^{(1)} &= \dot{\tau} v_B^{(1)} + \dot{V}, & S_2^{(1)} &= \dot{\tau} P^{(1)}, \\ S_2^{(2)} &= \dot{\tau} P^{(2)} - \dot{H}, \end{aligned} \quad (37)$$

with

$$P^{(m)} = \frac{1}{10} \left[\Theta_2^{(m)} - \sqrt{6} E_2^{(m)} \right]. \quad (38)$$

The modes with $m = -|m|$ satisfy the same equations with $B_\ell^{(-|m|)} = -B_\ell^{(|m|)}$ and all the other quantities unchanged.

These equations can be formally integrated, leading to simple expressions in terms of an integral along the line-of-sight [29]. The temperature fluctuations are given by

$$\frac{\Theta_\ell^{(m)}(\eta, k)}{2\ell+1} = \int_0^\eta d\eta' e^{-\tau} \sum_{\ell'} S_{\ell'}^{(m)}(\eta') j_\ell^{(\ell'm)}(k(\eta - \eta')), \quad (39)$$

where $j_\ell^{(\ell'm)}$ are given in ref. [29]. For the polarization, we have

$$\begin{aligned} \frac{E_\ell^{(m)}(\eta_0, k)}{2\ell+1} &= -\sqrt{6} \int_0^{\eta_0} d\eta \dot{\tau} e^{-\tau} P^{(m)}(\eta) \epsilon_\ell^{(m)}(k(\eta_0 - \eta)), \\ \frac{B_\ell^{(m)}(\eta_0, k)}{2\ell+1} &= -\sqrt{6} \int_0^{\eta_0} d\eta \dot{\tau} e^{-\tau} P^{(m)}(\eta) \beta_\ell^{(m)}(k(\eta_0 - \eta)), \end{aligned} \quad (40)$$

where the radial functions read

$$\begin{aligned} \epsilon_\ell^{(\pm 1)}(x) &= \frac{1}{2} \sqrt{(\ell-1)(\ell+2)} \left[\frac{j_\ell(x)}{x^2} + \frac{j'_\ell(x)}{x} \right], \\ \epsilon_\ell^{(\pm 2)}(x) &= \frac{1}{4} \left[-j_\ell(x) + j''_\ell(x) + 2 \frac{j_\ell(x)}{x^2} + 4 \frac{j'_\ell(x)}{x} \right], \end{aligned} \quad (41)$$

$$\begin{aligned} \beta_\ell^{(+1)}(x) &= -\beta_\ell^{(-1)}(x) = \frac{1}{2} \sqrt{(\ell-1)(\ell+2)} \frac{j_\ell(x)}{x}, \\ \beta_\ell^{(+2)}(x) &= -\beta_\ell^{(-2)}(x) = \frac{1}{2} \left[j'_\ell(x) + 2 \frac{j_\ell(x)}{x} \right]. \end{aligned} \quad (42)$$

Here the differential optical depth $\dot{\tau} = n_e \sigma_T a$ sets the collision rate in conformal time, with n_e the free electron density and σ_T the Thomson cross section and $\tau(\eta_0, \eta) \equiv \int_\eta^{\eta_0} \dot{\tau}(\eta') d\eta'$ the optical depth between η and the present time. The combination $\dot{\tau} e^{-\tau}$ is the *visibility function* and expresses the probability that a photon last scattered between $d\eta$ of η

and hence is sharply peaked at the last scattering epoch. In early reionization models, a second peak is also present at more recent times.

Scalar modes do not contribute to B-polarization, thus $B_\ell^{(0)} = 0$. We are interested in the contribution to the angular power-spectrum for the E and B modes arising from vector ($m = 1$) and tensor ($m = 2$) perturbations,

$$\begin{aligned} C_\ell^{(E)} &= \frac{2}{\pi} \int \frac{dk}{k} \sum_{m=-2}^2 k^3 \frac{|E_\ell^{(m)}(\eta_0, k)|^2}{(2\ell+1)^2}, \\ C_\ell^{(B)} &= \frac{2}{\pi} \int \frac{dk}{k} \sum_{m=-2}^2 k^3 \frac{|B_\ell^{(m)}(\eta_0, k)|^2}{(2\ell+1)^2}. \end{aligned} \quad (43)$$

A. Effects of decoupling

Before recombination, photons, electrons and baryons behave as a single tightly coupled fluid, so we can find approximate expressions for the polarization source $P^{(m)}$ using a perturbative expansion in inverse powers of the differential optical depth $\dot{\tau}$ ($k/\dot{\tau} \ll 1$) [36]. For the vector modes we need to consider the Euler equation for the velocity perturbation of baryons to close the system

$$\dot{v}_B^{(1)} = \dot{V} - \frac{\dot{a}}{a}(v_B^{(1)} - V) + \frac{\dot{\tau}}{R}(\Theta_1^{(1)} - v_B^{(1)}). \quad (44)$$

To leading order in the tight coupling approximation we obtain

$$\Theta_1^{(1)} = v_B^{(1)}, \quad (45)$$

and from the baryon Euler equation

$$v_B^{(1)} \simeq V. \quad (46)$$

To this perturbative order the quadrupole vanishes. However it does not vanish to the next order, and thus also $P^{(1)} \neq 0$. An appropriate expression for our calculation can be obtained by combining the equations for $\Theta_2^{(1)}$ and $E_2^{(1)}$ to obtain an evolution equation for $P^{(1)}$, and replacing in it the leading order solution we get

$$\dot{P}^{(1)} + \frac{3}{10}\dot{\tau}P^{(1)} - \frac{k}{10\sqrt{3}}V = 0. \quad (47)$$

This can be integrated to give

$$P^{(1)}(k, \eta) = \frac{k}{10\sqrt{3}} \int_0^\eta d\eta' V(k, \eta') \exp\left(-\frac{3}{10}\tau(\eta', \eta)\right). \quad (48)$$

Then, the B-mode polarization multipoles can be estimated by

$$\frac{B_\ell^{(1)}(\eta_0, k)}{2\ell+1} = -\frac{k\sqrt{2}}{10} \int_0^{\eta_0} d\eta \dot{\tau} e^{-\tau} \beta_\ell^{(1)}(k(\eta_0 - \eta)) \int_0^\eta d\eta' V(k, \eta') \exp\left(-\frac{3}{10}\tau(\eta', \eta)\right), \quad (49)$$

An analogous expression holds for $E_\ell^{(1)}$ replacing $\beta_\ell^{(1)}$ by $\epsilon_\ell^{(1)}$. Because of the sharpness of the visibility function around the time of decoupling η_D , $V(k, \eta')$ and $\beta_\ell^{(1)}(k(\eta_0 - \eta))$ (or $\epsilon_\ell^{(1)}$) can be evaluated at η_D and taken out of the integration. The remaining integral can be evaluated analytically approximating the visibility function by a Gaussian of width $\Delta\eta_D$ [36]

$$\frac{B_\ell^{(1)}(\eta_0, k)}{2\ell+1} = -\frac{k\sqrt{2}}{3} 0.51 \Delta\eta_D V(k, \eta_D) \beta_\ell^{(1)}(k(\eta_0 - \eta_D)). \quad (50)$$

Then, the resulting angular power-spectrum of B modes from vector perturbations results

$$C_\ell^{(B)(1)} = \frac{8}{9\pi} 0.51^2 \Delta\eta_D^2 \int dk k^4 \left[\beta_\ell^{(1)}(k(\eta_0 - \eta_D)) \right]^2 P_V(k, \eta_D), \quad (51)$$

where we have added the contribution coming from the $m = \pm 1$ modes. For $C_\ell^{(E)(1)}$ we obtain an analogous expression with $\epsilon_\ell^{(1)}(k(\eta_0 - \eta_D))$ replacing $\beta_\ell^{(1)}(k(\eta_0 - \eta_D))$. Replacing Eq. (22) we obtain

$$\frac{\ell(\ell+1)C_\ell^{(B)(1)}}{2\pi} = \ell(\ell+1) 16\frac{0.51^2}{25^2}\Delta_{\mathcal{R}}^4(k_0) \left(\frac{k_*}{k_0}\right)^{2(n_s-1)} C_V(n_s) \left(\frac{\Delta\eta_D}{\eta_0}\right)^2 \left(\frac{F(z_D)}{\eta_0}\right)^2 \eta_0 k_* \times \int dx x^2 (\beta_\ell^{(1)}(x))^2 W_V\left(\frac{x}{\eta_0 k_*}\right). \quad (52)$$

The integral can be conveniently evaluated using the WKB approximation for the Bessel functions appearing in $\beta_\ell^{(1)}$ and $\epsilon_\ell^{(1)}$, leading to

$$\langle (\beta_\ell^{(1)})^2(x) \rangle \simeq \frac{1}{8}(\ell-1)(\ell+2) \frac{1}{x^3 \sqrt{x^2 - \ell^2}} \quad (53)$$

$$\langle (\epsilon_\ell^{(1)})^2(x) \rangle \simeq \frac{1}{8}(\ell-1)(\ell+2) \left(\frac{1}{x^5 \sqrt{x^2 - \ell^2}} + \frac{\sqrt{x^2 - \ell^2}}{x^5} \right), \quad (54)$$

for $x > \ell$, and 0 for $x < \ell$. The results for the vector contribution to the B and E angular power-spectrum are shown in Figure 2, where we have used the following values for the parameters, for the concordance Λ CDM model ($\Omega_\Lambda = 0.7$, $\Omega_m = 0.3$, $\Omega_b h^2 = 0.022$, $h = 0.71$): $\Delta\eta_D/\eta_D = \Delta z_D/2z_D = 0.09$, $\eta_0/\eta_D = 30$, $k_* = 0.135 \text{ Mpc}^{-1}$ and $\Delta_{\mathcal{R}}^2(k_0) = 2.3 \times 10^{-9}$ at $k_0 = 0.002 \text{ Mpc}^{-1}$.

For the tensor modes, the tight coupling approximation to the leading order gives $P^{(2)} = \Theta_2^{(2)}/4 = -\dot{H}^{(2)}/3\dot{\tau}$. To the next order we obtain the following evolution equation for $P^{(2)}$

$$\dot{P}^{(2)} + \frac{3}{10}\dot{\tau}P^{(2)} + \frac{\dot{H}^{(2)}}{10} = 0, \quad (55)$$

that can be integrated

$$P^{(2)}(k, \eta) = -\frac{1}{10} \int_0^\eta d\eta' \dot{H}^{(2)}(k, \eta') \exp\left(-\frac{3}{10}\tau(\eta', \eta)\right). \quad (56)$$

Proceeding as for the vector case, we obtain for the B modes

$$\frac{B_\ell^{(2)}(\eta_0, k)}{2\ell+1} = \sqrt{\frac{2}{3}} 0.51 \Delta\eta_D \dot{H}^{(2)}(k, \eta_D) \beta_\ell^{(2)}(k(\eta_0 - \eta_D)). \quad (57)$$

and the same result changing $\beta_\ell^{(2)}$ by $\epsilon_\ell^{(2)}$ for the E modes.

Using Eq. (27) we can write

$$\dot{H}_S^{(2)}(k, \eta_D) = -3g_\infty^2 \frac{j_2(k\eta_D)}{\eta_D} \chi_S^{(2)}(k). \quad (58)$$

Then, for the angular power-spectrum, we obtain

$$\frac{\ell(\ell+1)C_\ell^{(B)(2)}}{2\pi} = \ell(\ell+1) \frac{12}{\pi^2} 0.51^2 \left(\frac{\Delta\eta_D}{\eta_D}\right)^2 g_\infty^4 \int dk k^2 \left[\beta_\ell^{(2)}(k(\eta_0 - \eta_D)) \right]^2 P_{\chi_S}(k) j_2^2(k\eta_D), \quad (59)$$

for the B modes (and the same expression with $\beta_\ell^{(2)} \rightarrow \epsilon_\ell^{(2)}$ for the E modes), with $P_{\chi_S}(k)$ given by Eq. (30). To perform the remaining integration it is convenient to use the WKB approximated expressions

$$\langle (\beta_\ell^{(2)})^2(x) \rangle \simeq \frac{1}{8} \left(\frac{\sqrt{x^2 - \ell^2}}{x^3} + \frac{4}{x^3 \sqrt{x^2 - \ell^2}} \right) \quad (60)$$

$$\langle (\epsilon_\ell^{(2)})^2(x) \rangle \simeq \frac{1}{8} \left[\left(1 - \frac{1 + \ell(\ell+1)/2}{x^2} \right)^2 \frac{1}{x \sqrt{x^2 - \ell^2}} + \frac{\sqrt{x^2 - \ell^2}}{x^5} \right],$$

for $x > \ell$, and 0 for $x < \ell$. The results are shown in Figure 2. The dominant contribution comes from the tensor modes for low multipoles, $\ell < 20$, while the vector contribution dominates for larger ℓ .

B. Effects of reionization

The recent detection by *WMAP* of excess power on large angular scales in the correlation between temperature and E-polarization of the CMB is a strong evidence that the Universe was reionized at relatively early times [37, 38]. The best fit to the Thomson scattering optical depth due to reionization is given by $\tau_{\text{ri}} = 0.17$, with still large uncertainties. In a spatially-flat Λ CDM model with $\Omega_\Lambda = 0.7$, reionization would have happened at a redshift $z_{\text{ri}} = 17$, if it took place in a single step.

Early reionization provides another opportunity for Thomson scattering to modify the polarization properties of the CMB. Its effects can be approximately decomposed in two parts [39]. On the one hand, rescattering damps already present anisotropies and polarization by a factor $e^{-\tau_{\text{ri}}}$. On the other hand, rescattering of the existing quadrupole anisotropy significantly enhances the polarization signal at low multipoles.

Here we estimate the effects of reionization on the polarization signal induced by secondary vector and tensor modes. We shall assume, for simplicity, that reionization took place in a single step. We can then approximate in Eq. (40) that the visibility function $\dot{\tau}e^{-\tau}$ is sharply peaked at η_{ri} and thus evaluate $\beta_\ell^{(m)}(k(\eta_0 - \eta))$ (and $\epsilon_\ell^{(m)}$) at $\eta = \eta_{\text{ri}}$ and take them out of the integral. The coupling between photons and electrons after reionization is, however, not very tight, and thus we can not proceed with the same approximations as in the previous section to compute the polarization sources $P^{(m)}(\eta)$. Indeed, $\dot{\tau} = -\sigma_T n_e a$ with $n_e = 0.88n_{b0}(1+z)^3 X(z)$ and $X(z)$ the ionization fraction. Thus $\dot{\tau} = 0.0019H_0(1+z)^2 X(z)(\Omega_b h^2/0.022)(0.71/h)$, and for the cosmological parameters under consideration, $k/\dot{\tau} \approx 0.5k\eta_0$ at $z = z_{\text{ri}}$, and the tight coupling approximation is not applicable at any relevant wavelength.

The polarization produced after reionization is essentially due to the scattering of existing quadrupole anisotropies, generated by scattering at earlier times or by gravitational effects during propagation. Since the quadrupole polarization E_2 generated during decoupling is typically smaller than the temperature quadrupole Θ_2 , we can approximate the polarization source as $P^{(m)} \approx \Theta_2^{(m)}/10$, and use for $\Theta_2^{(m)}$ the formal solution of Eq. (39), dropping in the fluctuation sources S of Eq. (37) the terms proportional to $\dot{\tau}$ against \dot{V} (in the case of vectors) or against \dot{H} (for the tensors), since the coupling is not tight.

The contribution of secondary vectors to B-polarization after reionization is then given by

$$\frac{B_\ell^{(1)}(\eta_0, k)}{2\ell + 1} = -\frac{\sqrt{6}}{2} \int_{\eta_{\text{ri}}}^{\eta_0} d\eta \dot{\tau} e^{-\tau} \beta_\ell^{(1)}(k(\eta_0 - \eta)) \int_0^\eta d\eta' \exp(-\tau(\eta', \eta)) \dot{V}(k, \eta') j_2^{(11)}(k(\eta - \eta')), \quad (61)$$

where $j_2^{(11)}(x) = \sqrt{3}j_2(x)/x$. For a single step reionization scenario, we can approximate

$$\frac{B_\ell^{(1)}(\eta_0, k)}{2\ell + 1} = -\frac{3}{\sqrt{2}} \Delta\eta_{\text{ri}} \dot{V}(k, \eta_{\text{ri}}) \beta_\ell^{(1)}(k(\eta_0 - \eta_{\text{ri}})) \frac{1}{k\eta_{\text{ri}}} \left(\frac{j_1(k\eta_{\text{ri}})}{k\eta_{\text{ri}}} - \frac{1}{3} \right). \quad (62)$$

We have defined an effective ‘‘reionization width’’ $\Delta\eta_{\text{ri}} \equiv \eta_{\text{ri}} \int_{\eta_{\text{ri}}}^{\eta_0} d\eta \dot{\tau} e^{-\tau}$, which for the $\Omega_m = 0.3$, spatially-flat Λ CDM model with single-step reionization and optical depth $\tau_{\text{ri}} = 0.17$ is $\Delta\eta_{\text{ri}} = 0.16\eta_{\text{ri}}$. This can be calculated taking into account that, for $z \leq z_{\text{ri}}$,

$$\tau(z) = 0.0042 \frac{\Omega_b h^2}{0.022} \frac{0.71}{h} \frac{0.3}{\Omega_m} \left(\sqrt{1 - \Omega_m + \Omega_m(1+z)^3} - 1 \right) \quad (63)$$

Notice that $\tau_{\text{ri}} = 0.17$ for $z_{\text{ri}} = 17$ if $\Omega_m = 0.3$. The reionization contribution to the power-spectrum of B-polarization by vector modes is finally approximately given by

$$\frac{\ell(\ell + 1)C_\ell^{(B)(1)}}{2\pi} = \ell(\ell + 1) \left(\frac{18}{25} \right)^2 \Delta_{\mathcal{R}}^4(k_0) \left(\frac{k_*}{k_0} \right)^{2(n_s - 1)} C_V(n_s) \left(\frac{\Delta\eta_{\text{ri}}}{\eta_{\text{ri}}} \right)^2 \left(\frac{F(z_{\text{ri}})}{\eta_{\text{ri}}} \right)^2 (\eta_0 - \eta_{\text{ri}}) k_* \int \frac{dx}{x^2} (\beta_\ell^{(1)}(x))^2 \left(\frac{j_1(y)}{y} - \frac{1}{3} \right)^2 W_V \left(\frac{x}{(\eta_0 - \eta_{\text{ri}})k_*} \right). \quad (64)$$

where $y = x\eta_{\text{ri}}/(\eta_0 - \eta_{\text{ri}})$. An analogous expression holds of course for $C_\ell^{(E)(1)}$ with $\epsilon_\ell^{(1)}$ in place of $\beta_\ell^{(1)}$.

The contribution of secondary tensor modes to the polarization induced after reionization can be estimated with similar approximations:

$$\frac{B_\ell^{(2)}(\eta_0, k)}{2\ell + 1} = -\frac{\sqrt{6}}{2} \int_{\eta_{\text{ri}}}^{\eta_0} d\eta \dot{\tau} e^{-\tau} \beta_\ell^{(2)}(k(\eta_0 - \eta)) \int_0^\eta d\eta' \exp(-\tau(\eta', \eta)) \dot{H}^{(2)}(k, \eta') j_2^{(22)}(k(\eta - \eta')), \quad (65)$$

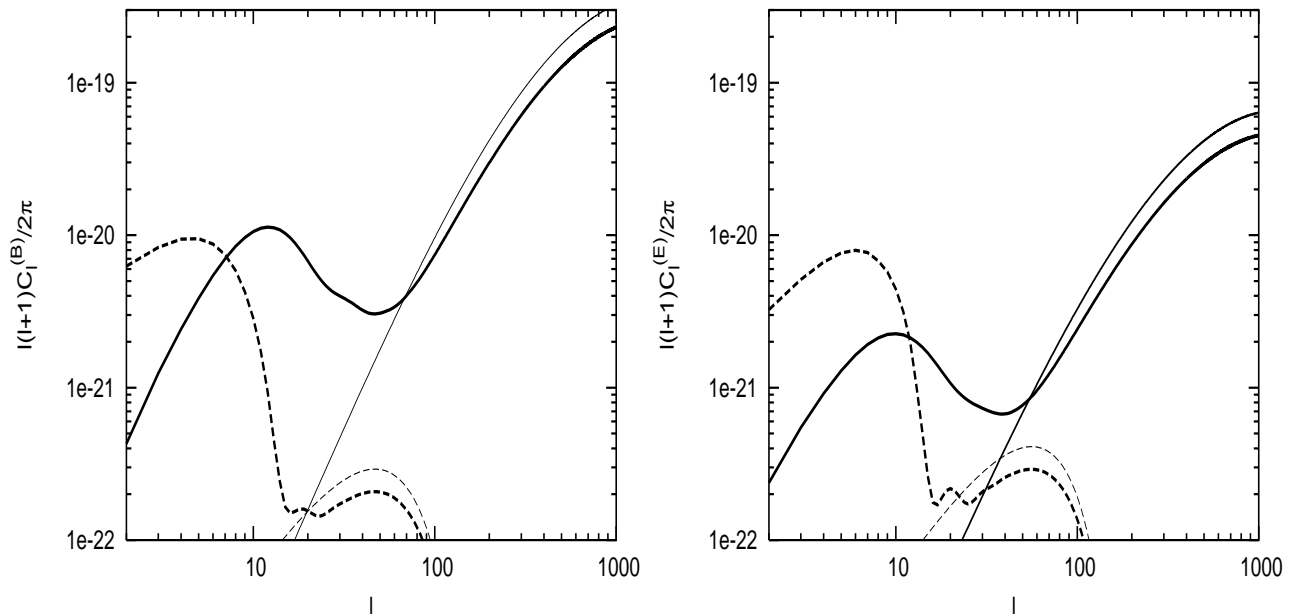


FIG. 2: Angular power-spectrum of B (left panel) and E (right panel) polarization by secondary vector (solid lines) and tensor modes (dashed lines), in a Λ CDM model without reionization (thin lines) and with an optical depth to reionization $\tau_{\text{ri}} = 0.17$ (thick lines).

where $j_2^{(22)}(x) = 3 j_2(x)/x^2$. We approximate

$$\frac{B_\ell^{(2)}(\eta_0, k)}{2\ell + 1} = -\frac{\sqrt{6}}{10} \Delta\eta_{\text{ri}}(1 + \delta) \dot{H}^{(2)}(k, \eta_{\text{ri}}) \beta_\ell^{(2)}(k(\eta_0 - \eta_{\text{ri}})) D(k\eta_{\text{ri}}). \quad (66)$$

We have defined an additional coefficient δ such that $\delta\Delta\eta_{\text{ri}} \equiv \int_{\eta_{\text{ri}}}^{\eta_0} d\eta \dot{\tau} e^{-\tau} \int_{\eta_{\text{ri}}}^{\eta} d\eta' e^{-\tau(\eta, \eta')}$. It accounts for the fact that in this case (opposite to the vector case) the time dependence of the source after reionization is not negligible. For the model parameters used throughout this work to estimate the effects, $\delta \approx 0.4$. The damping factor $D(x) \equiv 4/x$ if $x \leq 4$ (and $D = 1$ otherwise) arises because $j_2^{(22)}(x)$ can be approximated as $1/5$ only for small x ; larger values lead to oscillations that make the integral decay as $1/k$. Finally, the reionization contribution to the power-spectrum of B-polarization by secondary tensor modes is approximately given by

$$\frac{\ell(\ell+1)C_\ell^{(B)(2)}}{2\pi} = \ell(\ell+1) \frac{27}{25\pi^2} \left(\frac{\Delta\eta_{\text{ri}}}{\eta_{\text{ri}}} \right)^2 (1 + \delta)^2 g_\infty^4 \int dk k^2 \left[\beta_\ell^{(2)}(k(\eta_0 - \eta_{\text{ri}})) \right]^2 P_{\chi_s}(k) j_2^2(k\eta_{\text{ri}}) D^2(k\eta_{\text{ri}}). \quad (67)$$

The numerical result for the angular power-spectrum of E and B polarization by secondary vector and tensor modes produced after reionization, in the concordance Λ CDM model, is displayed in Fig. 2, added to the polarization that was produced during decoupling, damped by a factor $e^{-2\tau_{\text{ri}}}$.

IV. COMPARISON WITH PRIMARY TENSOR MODES AND COSMIC SHEAR

The signal from the secondary modes computed in the last section must be compared with the signal from the primordial gravitational-wave background generated during inflation. This depends on the model of inflation considered and its amplitude is parameterized by the 'tensor-to-scalar' ratio r (see Eq. (26)). Its angular power-spectrum can be accurately computed by available codes like CMBFAST [33], against which we have tested the accuracy of our semi-analytic approximations in the previous sections. The polarization induced by primordial gravitational waves can be calculated as in Eq. (59) replacing the power-spectrum of secondary modes $P_{\chi_s}(k)$ by that of the primary modes $P_{\chi_P}(k)$. The approximate expressions, both with or without reionization, are in good agreement (with more than 20% accuracy) with the numerical results obtained using CMBFAST. Notice that the polarization induced by primordial gravitational waves may be slightly smaller than it was calculated here due to damping by neutrino free-streaming [40], that we did not take into account.

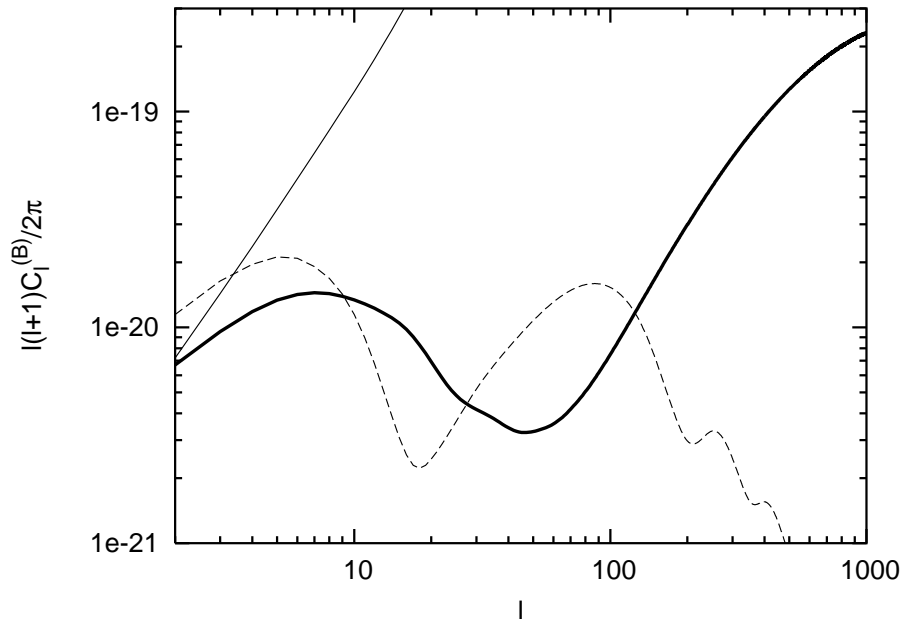


FIG. 3: Angular power-spectrum of secondary total (vector plus tensor) B-polarization (thick solid line) compared with that induced by primordial gravitational waves (dashed line) with a tensor to scalar ratio $r = 10^{-6}$, in a flat Λ CDM model ($\Omega_m = 0.3$) with $\tau_{\text{ri}} = 0.17$. The thin solid line is the signal due to gravitational lensing cleaned by a factor 40.

In Figure 3 we plot the numerical result (calculated with CMBFAST) for the B-polarization induced by primordial gravitational waves in a model with tensor to scalar ratio $r = 10^{-6}$, along with the total secondary B-modes (vector plus tensor) derived in this work. It is clear that the effects of primary and secondary modes are comparable. Primary modes have somewhat larger effects at the lowest ($\ell < 10$) multipoles, and also for ℓ between 30 and 100, but secondary modes overcome them in intermediate and larger values of ℓ . The power-spectrum induced by primordial gravitational waves scales as r . Thus, secondary vector and tensor fluctuations limit the ability to detect primordial gravitational waves through measurements of B-polarization if $r < 10^{-6}$.

The extraction of the B-polarization signature of primordial gravitational waves is seriously limited by weak gravitational lensing effects, that convert the dominant E-type polarization into B-modes [4], which swamp the signature of primordial tensor fluctuations unless they have a ratio to scalar fluctuations r of the order or larger than 10^{-4} . Fortunately, the weak lensing effect can be accounted for, through reconstruction of the gravitational lensing potential by the correlations of B-polarization between large and small angular scales, which primordial gravitational waves do not produce. “Cleaning” of the gravitational lensing signature may achieve factors of 40 in the power-spectrum, or even larger [10]. In Figure 3 we display the predicted gravitational lensing signal in B-polarization calculated with CMBFAST for the cosmological model under consideration, reduced by a factor 40. Clearly, an improvement in the cleaning algorithm would convert the secondary vector and tensor modes derived here in the barrier to the detection of primordial gravitational waves through B-polarization of the CMB if $r < 10^{-6}$.

V. CONCLUSIONS

The study of the magnetic-mode polarization of the CMB will become a fundamental and possibly unique tool to search for the stochastic gravitational-wave background, whose detection would represent a clear signature of a period of inflation in the early Universe. In contrast with temperature anisotropies and E-type polarization of the CMB, scalar perturbations do not give rise to B polarization in a direct way, so that measurements of the B-mode could be used to probe rather small gravitational-wave background amplitudes. Because of this reason, much observational effort is taking place for its detection, and future dedicated missions, such as NASA’s *Beyond Einstein* Inflation Probe [41] or ground-based experiments, like *BICEP* [42] and *PolarBeaR*, are being planned.

The main background for the detection of the B-mode is represented by the gravitational lensing conversion of a fraction of the dominant E-type into B-type polarization. However, it has been recently shown [10] that the lensing signal can largely be cleaned, thus allowing to probe inflationary models with tensor-to-scalar ratios $r \leq 10^{-6}$. As the

largest signal compared to the lensing one comes from low multipoles, where the reionization contribution is dominant, this limit depends on the Thomson scattering optical depth to reionization, that still has a large uncertainty.

At these sensitivity levels, there are other secondary effects that can give rise to sizable contributions to the B-type polarization. We estimated here the contribution coming from secondary vector and tensor modes, which originate by the mildly non-linear evolution of primordial density perturbations. The amplitude and harmonic content of this contribution is completely fixed, once the primordial power-spectrum of the density perturbations is known. For a concordance Λ CDM model, and adopting the high reionization redshift implied by the *WMAP* data [37, 38], we found that the effect of secondary vectors and tensors becomes comparable to that of primary gravitational waves for $r \leq 10^{-6}$, thus making it the actual background for the detection of primordial gravitational waves through B-mode polarization.

Acknowledgments

Work partially supported by ANPCyT, Fundación Antorchas and MIUR. We thank Paolo Natoli for discussions.

-
- [1] U. Seljak and M. Zaldarriaga, Phys. Rev. Lett. **78**, 2054 (1997); *ibid*, Phys. Rev. D **55**, 1830 (1997).
 - [2] M. Kamionkowski, A. Kosowsky and A. Stebbins, Phys. Rev. Lett. **78**, 2058 (1997); *ibid*, Phys. Rev. D **55**, 7368 (1997).
 - [3] R. R. Caldwell, M. Kamionkowski and L. Wadley, Phys. Rev. D **59**, 027101 (1999)
 - [4] M. Zaldarriaga and U. Seljak, Phys. Rev. D **58**, 023003 (1998)
 - [5] L. Knox and Y. S. Song, Phys. Rev. Lett. **89**, 011303 (2002).
 - [6] M. Kesden, A. Cooray and M. Kamionkowski, Phys. Rev. Lett. **89**, 011304 (2002).
 - [7] M. Kesden, A. Cooray and M. Kamionkowski, Phys. Rev. D **67**, 123507 (2003)
 - [8] W. H. Kinney, arXiv:astro-ph/0307005.
 - [9] C. M. Hirata and U. Seljak, arXiv:astro-ph/0306354.
 - [10] U. Seljak and C. M. Hirata, arXiv:astro-ph/0310163.
 - [11] W. Hu Astrophys. J. **529**, 12 (2000).
 - [12] T. R. Seshadri and K. Subramanian, Phys. Rev. Lett. **87**, 101301 (2001)
 - [13] K. Subramanian, T. R. Seshadri and J. D. Barrow, Mon. Not. Roy. Astron. Soc. **344**, L31 (2003).
 - [14] S. Mollerach and S. Matarrese, Phys. Rev. D **56**, 4494 (1997)
 - [15] S. Mollerach, Phys. Rev. D **57**, 1303 (1998)
 - [16] S. Matarrese, S. Mollerach and M. Bruni, Phys. Rev. D **58**, 043504 (1998).
 - [17] S. Mollerach, Phys. Rev. D **42** (1990) 313; K. Enqvist and M. S. Sloth, Nucl. Phys. B **626**, 395 (2002); D. H. Lyth and D. Wands, Phys. Lett. B **524**, 5 (2002); T. Moroi and T. Takahashi, Phys. Lett. B **522**, 215 (2001) [Erratum-*ibid*. B **539**, 303 (2002)].
 - [18] C. P. Ma and E. Bertschinger, Astrophys. J. **455**, 7 (1995).
 - [19] K. Tomita, Prog. Theor. Phys. **37**, 331 (1967).
 - [20] S. Matarrese, O. Pantano and D. Saez, Phys. Rev. Lett. **72**, 320 (1994)
 - [21] M. Bruni, S. Matarrese, S. Mollerach and S. Sonego, Class. Quant. Grav. **14**, 2585 (1997)
 - [22] F. C. Mena, R. Tavakol and M. Bruni, Int. J. Mod. Phys. A **17**, 4239 (2002)
 - [23] V. F. Mukhanov, H. A. Feldman and R. H. Brandenberger, Phys. Rept. **215**, 203 (1992).
 - [24] O. Lahav, P. B. Lilje, J. R. Primack and M. J. Rees, Mon. Not. Roy. Astron. Soc. **251**, 128 (1991).
 - [25] S. M. Carroll, W. H. Press and E. L. Turner, Ann. Rev. Astron. Astrophys. **30**, 499 (1992).
 - [26] N. Bartolo, S. Matarrese and A. Riotto, arXiv:astro-ph/0308088.
 - [27] V. Acquaviva, N. Bartolo, S. Matarrese and A. Riotto, Nucl. Phys. B **667**, 119 (2003).
 - [28] H. Noh and J. Hwang, arXiv:astro-ph/0305123.
 - [29] W. Hu and M. White, Phys. Rev. D **56**, 596 (1997).
 - [30] J. M. Bardeen, J. R. Bond, N. Kaiser and A. S. Szalay, Astrophys. J. **304**, 15 (1986).
 - [31] H. V. Peiris *et al.*, Astrophys. J. Suppl. **148**, 213 (2003).
 - [32] M. S. Turner, M. White and J. E. Lidsey, Phys. Rev. D **48**, 4613 (1993).
 - [33] U. Seljak and M. Zaldarriaga, Astrophys. J. **469**, 437 (1996).
 - [34] A. R. Liddle and D. H. Lyth, Phys. Lett. B **291**, 391 (1992); F. Lucchin, S. Matarrese and S. Mollerach, Astrophys. J. **401**, L49 (1992); R. L. Davis, H. M. Hodges, G. F. Smoot, P. J. Steinhardt and M. S. Turner, Phys. Rev. Lett. **69**, 1856 (1992) [Erratum-*ibid*. **70**, 1733 (1993)]; J. E. Lidsey, P. Coles, Mon. Not. Roy. Astron. Soc. **258**, 57P (1992); T. Souradeep and V. Sahni, Mod. Phys. Lett. A **7**, 3541 (1992).
 - [35] W. Hu, U. Seljak, M. White and M. Zaldarriaga, Phys. Rev. D **57** 3290 (1998).
 - [36] M. Zaldarriaga and D. D. Harari, Phys. Rev. D **52**, 3276 (1995).
 - [37] C. L. Bennett *et al.*, Astrophys. J. Suppl. **148**, 1 (2003).
 - [38] A. Kogut *et al.*, Astrophys. J. Suppl. **148**, 161 (2003).

- [39] M. Zaldarriaga, Phys. Rev. D **55**, 1822 (1997).
- [40] S. Weinberg, arXiv:astro-ph/0306304.
- [41] <http://universe.gsfc.nasa.gov>
- [42] <http://cosmology.berkeley.edu/group/swlh/bicep/>
- [43] Also, primordial gravitational waves give rise to second-order scalar and vector perturbations, but this effect is usually negligible [16].
- [44] Second-order Christoffel symbols can be found in Appendix A of Ref.[27] (see also [28]).
- [45] The relation with the inflation parameters is $\Delta_{\mathcal{R}}^2 = H^2/(\pi\epsilon m_P^2)$, with $m_P \equiv G^{-1/2}$